



PCCP

Control of Layer Stacking in CVD Graphene under Quasi-static Condition

Journal:	<i>Physical Chemistry Chemical Physics</i>
Manuscript ID:	CP-ART-06-2015-003541.R1
Article Type:	Paper
Date Submitted by the Author:	22-Jul-2015
Complete List of Authors:	Subhedar, Kiran; CSIR-National Physical Laboratory (NPL), New Delhi-12, India., Physics and Engineering of Carbon, Division of Materials Physics and Engineering and Academy of Scientific and Innovative Research (AcSIR)-NPL Sharma, Indu; CSIR-National Physical Laboratory (NPL), New Delhi-12, India., Physics and Engineering of Carbon, Division of Materials Physics and Engineering and Academy of Scientific and Innovative Research (AcSIR)-NPL Dhakate, Sanjay; CSIR-National Physical Laboratory (NPL), New Delhi-12, India., Physics and Engineering of Carbon, Division of Materials Physics and Engineering and Academy of Scientific and Innovative Research (AcSIR)-NPL

SCHOLARONE™
Manuscripts



Journal Name

ARTICLE

Control of Layer Stacking in CVD Graphene under Quasi-static Condition

Received 00th January 20xx,
Accepted 00th January 20xx

DOI: 10.1039/x0xx00000x

www.rsc.org/

Kiran M. Subhedar,^{*} Indu Sharma and Sanjay R. Dhakate

The type of layer stacking in bilayer graphene has significant influence on its electronic properties because of their contrast nature of layer coupling. Herein, different geometries of the reaction site for the growth of bilayer graphene by chemical vapor deposition (CVD) technique and their effect on the nature of layer stacking is investigated. The micro-Raman mapping and curve fitting analysis confirmed the type of layer stacking for the CVD grown bilayer graphene. The samples grown with sandwiched structure as quartz/Cu foil/quartz along with a spacer, between the two quartz plates to create a sealed space, resulted in Bernal or AB stacked bilayer graphene while the sample sandwiched without spacer produced the twisted bilayer graphene. The contrast difference in the layer stacking is consequence of the difference in the growth mechanism associated with different geometries of the reaction site. The diffusion dominated process under quasi-static control is responsible for the growth of twisted bilayer graphene in sandwiched geometry while surface controlled growth with ample and continual supply of carbon in sandwiched geometry along with a spacer lead to AB stacked bilayer graphene. Through this new approach, an efficient technique is presented to control the nature of layer stacking.

Introduction

Since its discovery, the single layer graphene is intriguing the scientific community with its extraordinary properties.¹⁻⁵ The possibility of the single layer graphene (SLG) growth with thermal chemical vapor deposition (CVD) technique became paradigm for high quality graphene synthesis, which offers viable technology for wafer scale production of graphene.⁶ Apart from SLG, CVD growth can yield bilayer graphene (BLG) or few layer graphene (FLG) with two types of layer stacking; first, AB or Bernal stacking, which is commonly present in the graphite and second one is the twisted stacking, where the individual graphene layers are rotationally stacked with some angle. Both of the types are equally important for application point view. The former one shows opening of tunable energy band gap under applied transverse electric field, which has applications in optics as a tunable lasers and in electronics as a transistor for logical switching device.⁷⁻⁹ The later with rotationally stacked layers depicts properties similar to SLG.¹⁰⁻¹² Moreover, it shows improved charge carrier mobility.¹³ Further, it has been observed that the rotationally stacked BLG decouples its electronic structure and preserves the intrinsic properties of SLG. When the twist angle between the stacked layers is more than 3 degrees, the charge carrier shows

characteristics of massless Dirac fermions, but with smaller carrier velocity and when this angle exceeds 20 degrees, the layers get completely decoupled, consequently its electronic properties become indistinguishable from the SLG.¹⁴ In the recent time, for graphene growth by CVD technique there has been worldwide interest in understanding the growth mechanism to find out the ways to control it.¹⁵⁻²² The self limiting effect of low pressure CVD growth of single layer graphene on copper vanishes when the set growth conditions are outside the optimized window and the percentage growth of SLG, BLG or FLG can vary with growth conditions.²³⁻²⁴ Usually such a CVD process results in mixture of AB stacked and twisted BLG and/or FLG. However, it remained significant challenge to experimentally control the growth process, which yields BLG predominantly having a one or other type of stacking, specially the twisted one. In light of this, in the present investigations we describe our results aimed to understand and control the CVD process for growth of BLG with exclusive rotational stacking. In order to confirm the formation of graphene and to reveal the information about layer stacking, an efficient tool, Raman Spectroscopy was employed. In thermal CVD for the growth of graphene on copper, the flux of carbon source plays significant role in the kinetics of graphene growth, which determines its quality and number of layers. Different geometries of reaction site for CVD growth of graphene were used to alter the flux of carbon source, which intern responsible for the number of layers and its relative orientation.

^a Physics and Engineering of Carbon, Division of Materials Physics and Engineering and

^b Academy of Scientific and Innovative Research (AcSIR)-NPL, CSIR-National Physical Laboratory (NPL), New Delhi-12, India.

^c *kmsubhedar@gmail.com, kms@nplindia.org

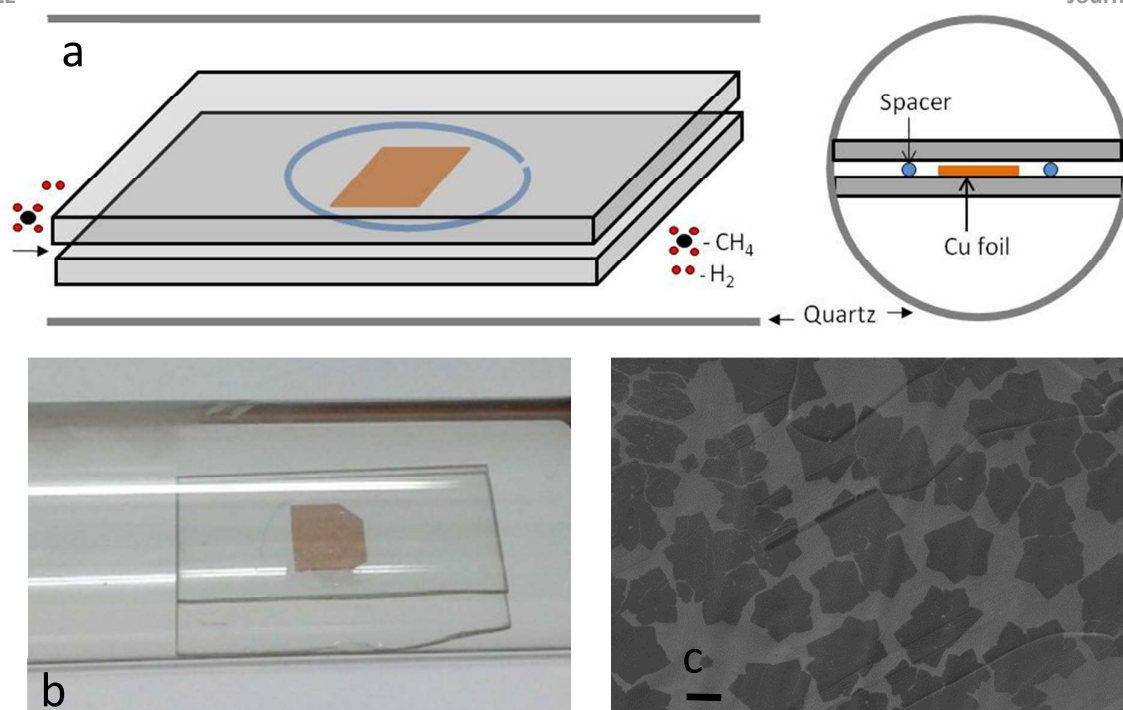


Figure 1. (a) Schematic representing Cu foil sandwiched between two quartz plates with platinum wire as spacer (b) Photograph (c) SEM image of CVD grown graphene domains on Cu foil with sandwiched geometry (scale bar-20 μ m)

Results and discussions

In addition to experimental conditions like flow of reactant gases, growth pressure, temperature, etc, the geometry of the reaction site has crucial role to play in the dynamics of the graphene growth. Here the reaction site is a macroscopic site where the hydrocarbon gets decomposed in the presence of catalyst and hydrogen at reaction temperature and further growth of the graphene on the substrate surface. In order to understand the nature of layer stacking of BLG and its control with CVD process, different sample geometries of the reaction site were explored as follows. In first case the Cu foil was sandwiched between two quartz plates, separated by the ring shaped platinum wire spacer having thickness more than the substrate copper foil, was used for the graphene growth so that there exists a space between the Cu foil and quartz plate as shown in the figure 1. The ring shape of the spacer makes an almost sealed space around the Cu foil, which helps to trap the Cu vapors flux and radicals of carbon source during the growth. In second case the Cu foil was kept as in first case, but without any spacer so that the surface of the Cu foil stays intimately in contact with quartz plate. The SEM image of the sample grown on Cu foil with this geometry is shown in figure 1(c). These sample geometries are referred as 'sandwiched with wire' and 'sandwiched' geometry, respectively and samples grown with above geometries are referred as S_w and S_{sd} , respectively.

Figure 2 (a,e) shows an optical micrograph of the graphene transferred onto the Si/SiO₂ wafer. The variation of color contrast in the optical micrograph²⁵ clearly indicates the BLG domain marked with blue sketch surrounded by single layer region as shown in figure 2a for the sample ' S_w '. Similarly, for sample ' S_{sd} ' consisting of bilayer and single-layer regions can be easily distinguished, which are outlined by inner and outer blue sketch in figure 2e. Raman spectroscopy has been extensively used to characterize the graphene, its quality or defect analysis, and the number of layers from characteristic peaks originating from different Raman active modes. Further, it gives significant and authentic information about layer stacking in case of BLG or FLG.²⁶⁻²⁷ The micro-Raman mapping together with contrast imaging can be used to study the uniformity of SLG, BLG or FLG and their relative orientations. The micro-Raman mapping was performed for the S_w , and S_{sd} samples at several locations and the representative results are presented in figure 2. The left panel shows (a) optical image of graphene, (b) Intensity, (c) peak width ($\Delta\omega$ cm⁻¹), (d) Peak position for 2D band in Raman mapping for the graphene grown with 'sandwiched with wire' geometry and the corresponding images (e-h) in the right panel represents 'sandwiched' sample S_{sd} . The Raman mapping of 2D band shows contrasting results for sample S_w , and S_{sd} . The 2D peak intensity at central BLG region of sample S_w is considerably less compared to the surrounding SLG area with noteworthy blue shift in its position compared to SLG region (figure 2b&d). The 2D band width gets almost doubled in the central BLG region compared to surrounded SLG region, which can be seen

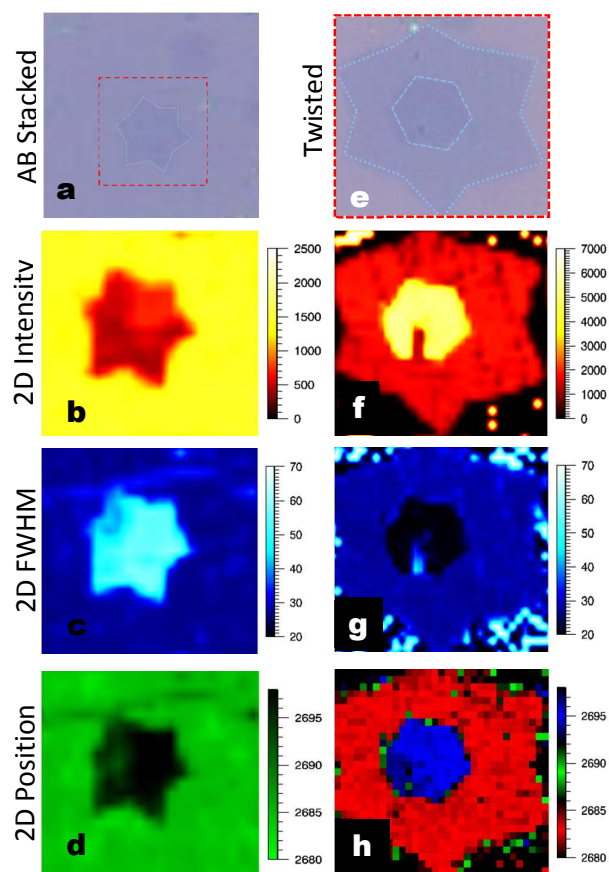


Figure 2. 2D band Raman mapping for different sample geometries. The left panel shows representative (a) optical image, (b) Intensity, (c) peak width FWHM ($\Delta\omega\text{cm}^{-1}$), (d) Peak position (ωcm^{-1}) for 2D band in Raman mapping for the graphene grown with 'sandwiched with wire' geometry and corresponding images (e - h) in the right panel shows data for 'sandwiched' sample S_{sd} . The scanned area with red dotted squares in the left panel is 20 by 20 μm and in the right panel 40 by 40 μm

clearly from the color contrast in image (figure 2c). These all are characteristic signatures of AB stacked BLG. For the sample S_{sd} with 'sandwiched' geometry, the 2D band intensity in the inner smaller BLG domain raises up four times compared to outer SLG area with blue shift in its position, which indicates the twisted nature of BLG. However, it is surprising to see that there is no broadening of the 2D band in contrast to earlier studies.²⁸ In fact the 2D peak width in BLG region remains close to the single layer values (figure 2g). This is due to complete decoupling of layers with higher twist angle.^{14,29}

The shape and intensity of the 2D peak are characteristically different for SLG, AB stacked and twisted BLG. Hence, to ensure the nature of layer stacking in CVD grown BLG, the analysis of curve fitting for 2D peak was performed. Figure 3 shows Raman spectra recorded at (a) BLG domain in the sample S_w , (b) single layer region and (c) bilayer region for graphene domain in sample, S_{sd} in the left panel.

The result of curve fitting of the corresponding 2D peak for (d) AB-stacked BLG in sample S_w grown with 'sandwiched with wire' geometry (e) SLG and (f) twisted BLG with 'sandwiched' geometry is shown in the right panel. The Raman spectra recorded in the single layer region in the sample S_{sd} is typical of SLG with I_{2D}/I_G ratio around 3 and narrow 2D peak having the width around ~ 29 , which fits with single peak (figure 3b,e). However, in case of spectra recorded at central BLG region, the 2D peak fits with single peak, but with blue shift in its peak position and with the substantial increase in I_{2D}/I_G ratio (figure 3c,f) because of decoupling of its electronic structure.^{14,29} This clearly means in the central BLG domain, the two layers are twisted with each other. According to the theoretical calculation and experimental data²⁹ the shift in 2D peak position, Intensity and FWHM of 2D peak varies systematically with its twist angle and it remains constant after 20° i.e the I_{2D} remains constant at a value double than that of the single layer, blue shift in the 2D peak position remain at about 12cm^{-1} and its FWHM remains at around value that of the single layer. The values of these parameters in the present investigation is compared with theoretical calculations and experimental data in reference 29 and it is confirmed that the layers are twisted with each other and the angle of the twist is more than 20° . Further, the optical image of sample S_{sd} in figure 3, the SLG and BLG are clearly distinguished from its color contrast. Hence it is possible to calculate the angle between facets in case of domains with proper hexagonal shape. However, there are few domains found where it is difficult to see the facets clearly and calculate its angle exactly but still they are twisted as inferred from Raman studies. So out of about 80% twisted BLG domains, 60% domains have twist angle of $30^\circ(\pm 2)$ and rest of the 20% domains have angle between 20 to 30° . Hence, the twisted BLG growth is dominated with BLG domains with twist angle $30^\circ(\pm 2)$. This value of estimated twist angle is energetically more favorable because it is next lowest energy structure (1.6eV/atom) with twisted stacking after the most stable AB stacking.³⁰

In case of BLG from sample S_w , the I_{2D}/I_G ratio is less than 2 and the 2D peak has broad $\Delta\omega$ of 55 and fits with cumulative peak having four components, each with $\Delta\omega$ of 30, 29, 30 and 33, respectively and middle two peaks have higher intensities compared to other two (figure 3a,d). This result is in well agreement with the fact that the 2D peak in Raman spectra of AB stacked BLG has four components $2D_{1B}$, $2D_{1A}$, $2D_{2A}$, $2D_{2B}$, originating from a two phonon double resonance Raman process,³¹ two of which, $2D_{1A}$ and $2D_{2A}$, have higher intensities.²⁶ This confirms AB stacking of the layers in BLG for sample S_w .

Raman spectra were recorded for 8-9 samples of each condition for the analysis of curve fitting and intensity ratio to get information about layer stacking from Raman studies. For each of the sample the spectra were recorded at 4-5 different locations in the sample. Out of this, 2-3 samples from each condition were studied for micro Raman measurements. About 80% of the samples of each condition show the respective layer stacking i.e AB or twisted stacking as discussed above. Thus the analysis of Raman mapping and peak fitting of

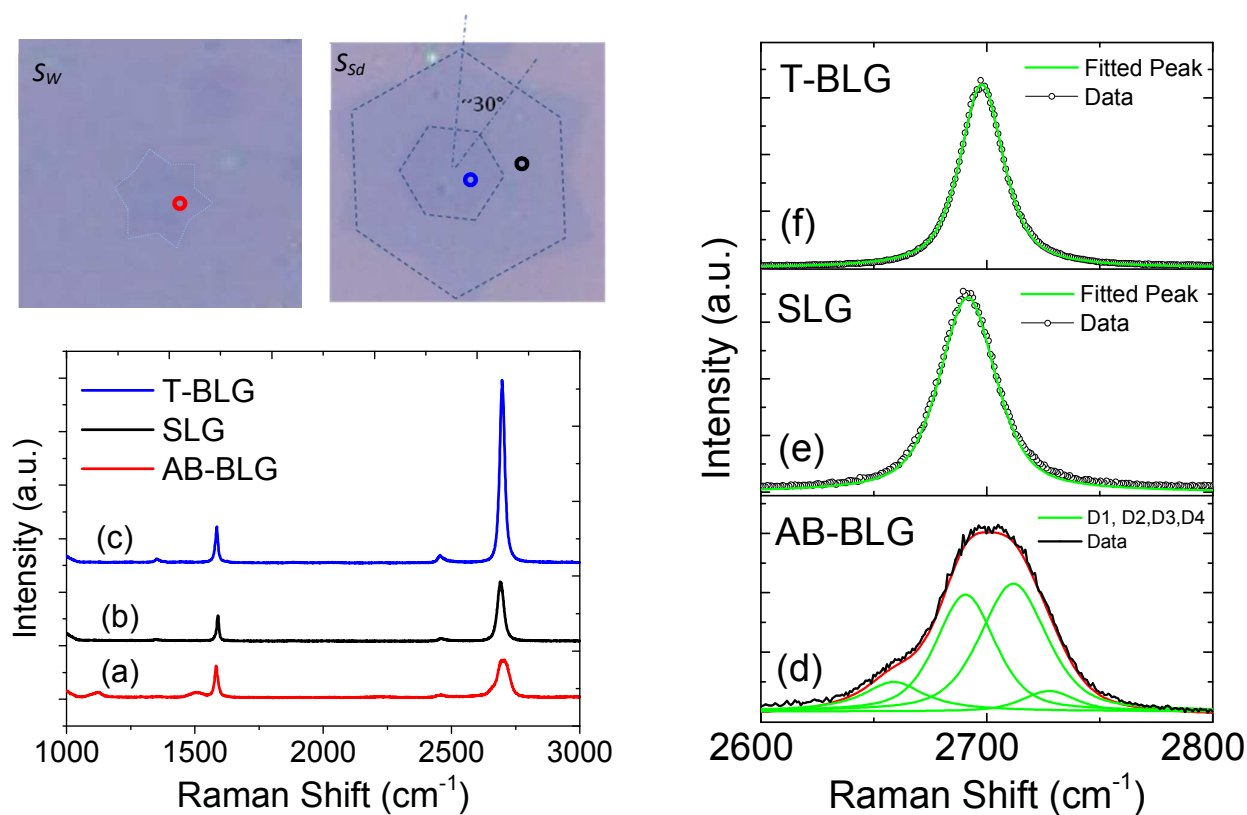


Figure 3. Raman Spectra of (a) BLG domain in the sample S_W (b) single layer region and (c) bilayer region for graphene sample, S_{Sd} . The curve fitting of the corresponding 2D peak for (d) AB stacked sample S_W grown with 'sandwiched with wire' geometry (e) SLG and (f) twisted BLG with 'sandwiched' geometry

2D band, unambiguously confirmed that the sample with 'sandwiched with wire' geometry results in AB stacked BLG and with 'sandwiched' geometry yields twisted BLG. This contrast difference in layer stacking is believed to be coming from the different kind of growth mechanism associated with different geometries. The typical low pressure CVD growth of graphene on copper is self limiting process dominated by surface controlled growth as carbon from catalytically cracked source covers the Cu surface, forms monolayer and passivates the catalytic activity of Cu surface, which inhibits the further growth and process get restricted to monolayer. However, this is valid only for optimum and continual supply of carbon. The enclosure geometry was introduced by Li *et al.* for the growth of large size domains.³² The method was further used to grow the BLG and found that the growth of BLG occurs on outside of the enclosure because of the delayed passivation of Cu from inside, leading diffusion of carbon from inside to outside through the Cu foil of the enclosure and the proposed mechanism based on evidence revealed it as a diffusion controlled process.^{17,18} On the contrary, different mechanism proposed again based on the evidence suggested that the growth of SLG/BLG on copper, could be a surface phenomena^{15,16} or even layer by layer epitaxial growth from top.²³ The growth process employed in these reports suggests that the sample geometry has its pronounced effect on the

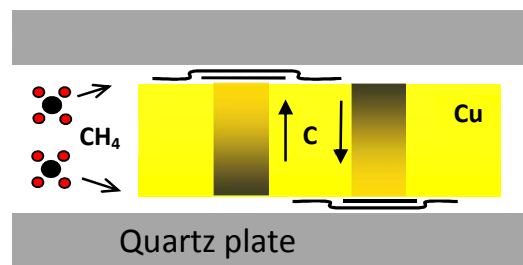


Figure 4. Schematic illustrating the growth mechanism of BLG with 'sandwiched' geometry

growth mechanism for growth of BLG.

In the present case, for the sample with 'sandwiched' geometry, the Cu substrate is sandwiched between the quartz plates, where the Cu surface is intimately in contact with quartz surface and there is no direct flow of reactant gas over the Cu surface. However, as illustrated by the mechanism in figure 4, the gases can leak in between Cu surface and quartz surface with a very slow rate, which reduces the supply of carbon source and creating a quasi-static distribution of reactant gases, which makes delay in surface coverage of Cu with monolayer graphene. Subsequently, with the time Carbon

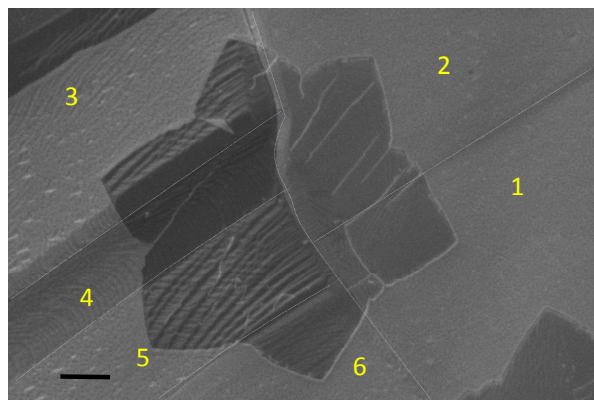


Figure 5. SEM of graphene domain grown across the different facets and grain boundary of Cu (scale bar -5 μ m)

get diffuse through bulk of the Cu foil and reach other side of the foil, where it grows second layer underneath the top layer and form the BLG similar to the enclosure growth method,¹⁷ but with a significant difference that here, the Cu foil is sandwiched between the two quartz plates, making the BLG growth exclusively under diffusion control because neither of the Cu side is directly exposed to flow of the gases. This is very important as all the BLGs grown will have similar kind of growth environment and process. Further, adding a second layer from beneath requires debonding of first layer; the weak interaction between Cu and graphene favors this debonding.³³ The weak nature of this interaction can be inferred from observation of graphene domains growing without impediment across facets and copper grain boundaries as shown in figure 5 and from theoretical work that found a weak electronic interaction between graphene and Cu, manifested by preservation of the Dirac cones.³⁴ It is also reported that the growth of second layer from below prefers the first layer, which is rotated with respect to the substrate orientation because of its weak bonding.³⁵ This kind of graphene growth of second layer on the copper has many rotational variants because of its weak interactions with Cu. Neither substrate nor the overlying graphene strongly locks the underneath second layer in to same orientation as the overlying first graphene layer, leading to BLG with twisted stacking.³⁶ Hence, the twisted layer stacking of BLG in our sample with sandwiched geometry is originating from exclusive diffusion controlled process under quasi-static control and weak interactions of graphene with Cu.

In case of 'sandwiched with wire' geometry because of the spacer, the Cu surface is not intimately in contact with quartz surface. Hence, the reactant gases can enter relatively easy inside the closed space formed because of the spacer, where the extra carbon radicals or fragments generated from methane in the presence of trapped Cu vapor flux³⁷ inside the closed space get adsorbed on monolayer graphene, which usually get covered in initial short time. The proposed mechanism is illustrated in figure 6. This could lead to growth of second layer graphene from top on the fast grown first

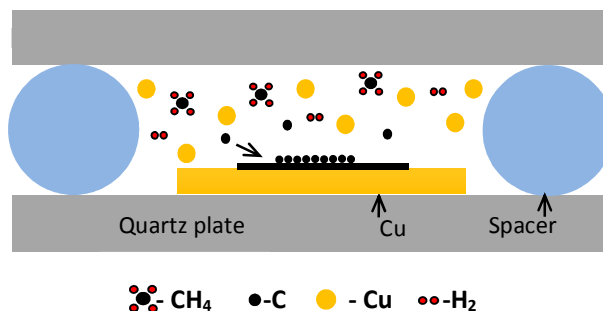


Figure 6. Schematic illustrating the growth mechanism of BLG with 'sandwiched with wire' geometry

layer. Consequently, the growth of BLG is dominated with AB stacking and underlying mechanism could be the surface controlled growth. It is reasonable to accept this growth mechanism as it is consistent with the earlier reports, where they adopted a similar kind of approach to grow the second layer epitaxially from top on already grown monolayer graphene with the aid of additional fresh Cu foil as a catalyst to create an extra carbon flux for the growth of second layer.²³⁻²⁴

The contrast nature of layer stacking for samples with different geometries of reaction site suggests its different underlying growth mechanisms, originating from the process which supplies the extra carbon flux, needed for second layer *i.e.* by diffusion through Cu foil or from the top in the presence of Cu vapor flux. The different geometries of reaction site dictate the nature BLG growth process, which is either dominated with diffusion controlled or surface control mechanism, which in intern responsible for different stacking of BLG.

The CVD process employed in the present investigations yields sample with good uniformity. The size of the Cu foil or substrate used for the CVD growth is 20 x 20 mm and the growth is consistently uniform all over the substrate except at edges where about 1mm there is non-uniform growth and uncovered regions were observed. Further, large area samples can be grown using CVD system with quartz reactor with larger diameter. In case of 'sandwiched with wire' growth for AB stacked BLG, the trapping of the Cu vapor is very crucial. It will help to supply source carbon even after the coverage of single layer graphene. Proper diameter of the spacer wire for efficient trapping of Cu vapors, flow rate of the reactant gases and temperature are the crucial parameter needed to tune good yield.

Sample S_W and S_{Sd} , sometime in contrast results in twisted and AB stacked BLG, respectively, which is very rare. At some places occasionally it grows graphene more than two layers. Overall the S_W geometry is dominated with AB stacked and S_{Sd} geometry is dominated with twisted BLG.

Conclusions

Different geometries of the reaction site for the growth of BLG and their effect on the nature of layer stacking is

demonstrated. The Raman mapping and curve fitting analysis confirmed the type of layer stacking for the BLG grown by CVD technique. The sample grown with sandwiched structure as quartz/Cu foil/quartz along with a spacer, between the two quartz plates to create a sealed space, resulted in AB stacked BLG, while the sandwiched geometry without spacer yields samples with twisted BLG. This contrast difference in layer stacking is consequence of the difference in the growth mechanism associated with different geometries of the reaction site. The diffusion dominated process under quasi-static control created with the aid of the sandwiched structure lead to the growth of twisted BLG while surface controlled growth with ample and continual supply of carbon created with the aid of sandwiched structure with spacer lead to AB stacked BLG. Through this new approach, an efficient technique to control the layer stacking of BLG grown by CVD is presented, which can be used to tailor its electronic properties. The present study will advance the understanding of stacking control in graphene growth with CVD, which is important for technological applications that rely either on energy gap and high carrier mobility of the graphene, like electronic switching devices or graphene r.f. transistors. This will allow for a more efficient engineering of bilayer graphene. Junctions between twisted and Bernal-stacked BLG could also enable novel heterostructure devices.

Experimental Section

Prior to graphene growth, 25 μm thick copper foil (99.8% Cu, Alfa Aesar #13382) was thoroughly cleaned with acetone, acetic acid, DI water and IPA. The copper foil was placed inside a quartz reactor at an isothermal zone of a custom built thermal CVD system and evacuated, filled with argon and again pumped down to 0.005 mbar, then heated to 1045 $^{\circ}\text{C}$ under hydrogen flow of 12 sccm. Hydrogen flow was reduced to 8 sccm and kept for annealing for 20 min to increase grain growth /crystallinity of the Cu foil and remove the thin oxide layer grown on it. Subsequently, for the growth of graphene the methane was introduced with flow rate of 4 sccm for initial time period of 3 minutes followed by increase in its flow rate to 25 sccm with total growth time of 30 minutes. After growth the samples were cooled down quickly by sliding the furnace. Methane flow was turned off at 650 $^{\circ}\text{C}$ and hydrogen below 100 $^{\circ}\text{C}$. The pressure inside CVD reactor during the growth was about 0.130 and 0.4 mbar, respectively, for first 3 min and rest of the growth. In order to transfer the CVD grown graphene on silicon wafer, PMMA solution (molecular weight 495000 g/mol, 4% by volume dissolved in anisole) was spin coated onto the top side of the sample at 3000 rpm and dried overnight, subsequently, was put in 20% ammonium persulphate (APS) etchant solution in deionized water as a copper etchant for two hours followed by additional etching with fresh etchant for 12 hours to ensure the complete etching of copper. After the etching step the PMMA supported graphene was rinsed with deionized water several times before scoop out with substrate. The PMMA was finally removed with warm acetone. The silicon substrates used in this work were highly p-doped

and with 300 nm thermal oxide on top. The micro-Raman mapping was performed under ambient conditions with a Renishaw InVia micro-Raman spectrometer equipped with a 514 nm (2.41eV) wavelength excitation laser and 2400 lines/mm grating. A laser beam size of $\sim 1 \mu\text{m}$ with $\times 50$ objective lens is used.

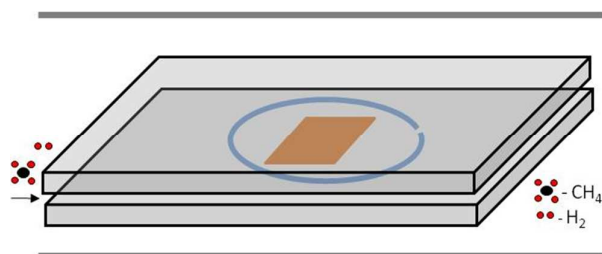
Acknowledgements

Authors are thankful to CSIR for supporting this work. One of the authors IS would like thanks CSIR for granting Senior Research fellowship.

References

- 1 K. S. Novoselov, A. K. Geim, S. V. Morozov, D. Jiang, Y. Zhang, S. V. Dubonos, I. V. Grigorieva, A. A. Firsov, *Science* **2004**, 306, 666.
- 2 K. S. Novoselov, A. K. Geim, S. V. Morozov, D. Jiang, M. I. Katsnelson, I. V. Grigorieva, S. V. Dubonos, A. A. Firsov, *Nature* **2005**, 438, 197.
- 3 A. K. Geim, K. S. Novoselov, *Nat. Mater.* **2007**, 6, 183.
- 4 Zacharias G. Fthenakis and Nektarios N. Lathiotakis, *Phys. Chem. Chem. Phys.* **2015**, 17, 16418
- 5 Wang Yong, Zhang Xue-Qing and Li Hui, *Chinese Phys. Lett.* **2014**, 31, 117201
- 6 X. S. Li, W. W. Cai, J. H. An, S. Kim, J. Nah, D. X. Yang, R. Piner, A. Velamakanni, I. Jung, E. Tutuc, S. K. Banerjee, L. Colombo, R. S. Ruoff, *Science* **2009**, 324, 1312.
- 7 C. H. Lui, Z. Li, K. F. Mak, E. Cappelluti, T. F. Heinz, *Nat. Phys.* **2011**, 7, 944.
- 8 E. Castro, K. Novoselov, S. Morozov, N. Peres, J. dos Santos, J. Nilsson, F. Guinea, A. Geim and A. Neto, *Phys. Rev. Lett.* **2007**, 99, 216802.
- 9 Y. Zhang, T.T. Tang, C. Girit, Z. Hao, M. C. Martin, A. Zettl, M. F. Crommie, Y. R. Shen and F. Wang, *Nature* **2009**, 459, 820.
- 10 J. Hass, F. Varchon, J. E. Milla'n-Otaya, M. Sprinkle, N. Sharma, W. A. de Heer, C. Berger, P. N. First, L. Magaud, and E. H. Conrad, *Phys. Rev. Lett* **2008**, 100, 125504
- 11 J. M. B.Lopes dos Santos, N. M. R. Peres, A. H. Castro, *Phys. Rev. Lett.* **2007**, 99, 256802.
- 12 M. Sprinkle, D. Siegel, Y. Hu, J. Hicks, A. Tejada, A. Taleb-Ibrahimi, P. Le Fe`vre, F. Bertran, S. Vizzini, H. Enriquez, S. Chiang, P. Soukiassian, C. Berger, W. A. de Heer, A. Lanzara and E. H. Conrad, *Phys. Rev. Lett.* **2009**, 103, 226803
- 13 Bruno Dlubak, Marie-Blandine Martin, Cyrille Deranlot, Bernard Servet, Stéphane Xavier, Richard Mattana, Mike Sprinkle, Claire Berger, Walt A. De Heer, Frédéric Petroff, Abdelmadjid Anane, Pierre Seneor and Albert Fert, *Nat. Physics* **2012**, 8, 557.
- 14 A. Luican, G. H. Li, A. Reina, J. Kong, R. R. Nair, K. S. Novoselov, A. K. Geim and E. Y. Andrei, *Phys. Rev. Lett.* **2011**, 106, 126802.
- 15 X. Li, W. Cai, L. Colombo and R. S. Ruoff, *Nano Lett.* **2009**, 9, 4268.
- 16 X. Li, Carl W. Magnuson, Archana Venugopal, Jinho An, Ji Won Suk, Boyang Han, Mark Borysiak, Weiwei Cai, Aruna Velamakanni, Yanwu Zhu, Lianfeng Fu, Eric M. Vogel, Edgar Voelkl, Luigi Colombo, and R. S. Ruoff, *Nano Lett.* **2010**, 10, 4328.
- 17 W.J. Fang, A.L. Hsu, Y. Song, A.G. Birdwell, M. Amani, M. Dubey, M.S. Dresselhaus, T Palacios., J. Kong and J. Kong, *ACS Nano* **2014**, 8, 6491

- 18 W. Fang, A. L. Hsu., R. Caudillo, Y Song., A. G. Birdwell, E. Zakar, M. Kalbac, M. Dubey, T. Palacios, M. S. Dresselhaus, *Nano Lett.* **2013**, 13, 1541.
- 19 Sreekar Bhaviripudi, Xiaoting Jia, Mildred S. Dresselhaus, Jing Kong, *Nano Lett.* **2010**, 10, 4128.
- 20 I. Vlassiouk, M. Regmi, P. Fulvio, S. Dai, P. Datskos, G. Eres and S. Smirnov, *ACS Nano* **2011**, 5, 6069.
- 21 B. Wu, D. Geng, Z. Xu, Y. Guo, L. Huang, Y. Xue, J. Chen, G. Yu and Y. Liu, *NPG Asia Mater.* **2013**, 5, e36.
- 22 Yingfeng Li, Meicheng Li, Tai Wang, Fan Bai and Yang-Xin Yu, *Phys. Chem. Chem. Phys.* **2014**, 16, 5213
- 23 K. Yan, H. Peng, Y. Zhou, H. Li and Z. Liu, *Nano Lett.* **2011**, 11, 1106.
- 24 L. Liu, H. Zhou, R. Cheng, W. J. Yu, Y. Liu, Y. Chen, J. Shaw, X. Zhong, Y. Huang and X. Duan, *ACS Nano.* **2012**, 6, 8241.
- 25 P. Blake, E. W. Hill, A. H. C. Neto, K. S. Novoselov, D. Jiang, R. Yang, T. J. Booth and A. K. Geim, *Appl. Phys. Lett.* **2007**, 91, 063124.
- 26 A. C. Ferrari, J. C. Meyer, V. Scardaci, C. Casiraghi, M. Lazzeri, F. Mauri, S. Piscanec, D. Jiang, K. S. Novoselov, S. Roth and A. K. Geim, *Phys. Rev. Lett.* **2006**, 97, 187401.
- 27 P. Poncharal, A. Ayari, T. Michel and J. L Sauvajol. *Phys. Rev. B* **2008**, 78, 113407.
- 28 P. Lespade and André Marchand. *Carbon* **1984**, 22, 375 Cross reference from. A. C. Ferrari, and D. M. Basko, *Nat. Nanotechnol.* **2013**, 8, 235.
- 29 K. Kim, S. Coh, L. Z. Tan, W. Regan, J. M. Yuk, E. Chatterjee, M. F. Crommie, M. L. Cohen, S. G. Louie and A. Zettl, *Phys. Rev. Lett.* **2012**, 108, 246103
- 30 S. Shallcross, S. Sharma and O. A. Pankratov, *J. Phys.:Condens. Matter* **2008**, 20, 454224.
- 31 C. Thomsen and S. Reich, *Phys. Rev. Lett.* **2000**, 85, 5214
- 32 X. S. Li, C. W. Magnuson, A. Venugopal, R.M. Tromp, J.B. Hannon, E. M. Vogel, L. Colombo and R. S. Ruoff, *J. Am. Chem. Soc.* **2011**, 133, 2816.
- 33 H. Chen, W. G. Zhu and Z. Y. Zhang, *Phys. Rev. Lett.* **2010**, 104, 186101
- 34 P. A. Khomyakov, G. Giovannetti, P. C. Rusu, G. Brocks, J. van den Brink and P. J. Kelly, *Phys. Rev. B.* **2009**, 79, 195425.
- 35 S. Nie, A. L. Walter, N. C. Bartelt, E. Starodub, A. Bostwick, E. Rotenberg and K. F. McCarty, *ACS Nano.* **2011**, 5, 2298.
- 36 S. Nie, W. Wu, S. Xing, Q. Yu, J. Bao, S. Pei and K. F. McCarty, *New J. Phys.* **2012**, 14, 093028.
- 37 Hung-Chiao Lin, Yu-Ze Chen, Yi- Chung Wang and Yu-Lun Chueh, *J. Phys. Chem. C* **2015**, 119, 6835.



For Table of Contents entry

